Local Quantification of Wall Thickness and Intraluminal Thrombus Offer Insight into the Mechanical Properties of the Aneurysmal Aorta

Giampaolo Martufi,[1] Alessandro Satriano,[2] Randy D. Moore,[3] David A. Vorp,[4,5] and Elena S. Di Martino[1,6]

[1]Department of Civil Engineering, Schulich School of Engineering, University of Calgary, 2500 University Drive NW, Calgary, AB T2N 1N4, Canada; [2]Department of Cardiac Sciences, University of Calgary, Calgary, Canada; [3]Department of Surgery, University of Calgary, Calgary, Canada; [4]Departments of Bioengineering and Surgery, University of Pittsburgh, Pittsburgh, USA; [5]McGowan Institute for Regenerative Medicine, University of Pittsburgh, Pittsburgh, USA; and [6]Centre for Bioengineering Research and Education, University of Calgary, Calgary, Canada

Associate Editor Umberto Morbiducci oversaw the review of this article.

Abstract—Wall stress is a powerful tool to assist clinical decisions in rupture risk assessment of abdominal aortic aneurysms. Key modeling assumptions that influence wall stress magnitude and distribution are the inclusion or exclusion of the intraluminal thrombus in the model and the assumption of a uniform wall thickness. We employed a combined numerical-experimental approach to test the hypothesis that abdominal aortic aneurysm (AAA) wall tissues with different thickness as well as wall tissues covered by different thrombus thickness, exhibit differences in the mechanical behavior. Ultimate tissue strength was measured from *in vitro* tensile testing of AAA specimens and material properties of the wall were estimated by fitting the results of the tensile tests to a histo-mechanical constitutive model. Results showed a decrease in tissue strength and collagen stiffness with increasing wall thickness, supporting the hypothesis of wall thickening being mediated by accumulation of non load-bearing components. Additionally, an increase in thrombus deposition resulted in a reduction of elastin content, collagen stiffness and tissue strength. Local wall thickness and thrombus coverage may be used as surrogate measures of local mechanical properties of the tissue, and therefore, are possible candidates to improve the specificity of AAA wall stress and rupture risk evaluations.

Keywords—Computational mechanics, Aneurysm, Imaging.

INTRODUCTION

Abdominal aortic aneurysm (AAA) is defined as a localized dilatation of the abdominal aorta resulting from a multifactorial process that culminates in an irreversible pathological remodeling of the aortic wall. The overall result is a gradual imbalance between synthesis and degradation of tissue constituents leading to the loss of structural integrity of the aortic wall.[7] Aneurysms are often asymptomatic and if left untreated may progress toward further enlargement and rupture at any point in time regardless of their size or age of the pathology, with high mortality risks.[44] Current clinical estimates of rupture risk are based on measures of maximum diameter and diameter growth rate. However, the use of size only as a guide to inform decisions of elective repair has faced strong challenge because of its inability to accurately predict rupture for all AAAs.[4,6,9,13,17,33,43] Mathematically derived mechanics-based indices have been proposed as improved predictors of AAA rupture, namely peak wall stress (PWS; the maximum stress in the wall) and rupture potential index (RPI; the local stress/strength ratio in the wall).[10,14,45,46] Computing these indexes involves the use of finite element analysis (FEA) techniques and requires several modeling assumptions that affect the results of the analysis.[14,29,39] Key modeling assumptions that influence AAA wall stress magnitude and distribution are the inclusion or exclusion of the intraluminal thrombus (ILT) and the assumption of a uniform wall thickness.[29] Pathology specimens demonstrated that the aortic wall thickness vary significantly across different patients, as well as within each individual aneurysm.[8,35] Due to the inability to measure thickness noninvasively, a uniform wall thickness is typically assumed in the vast majority of biomechanical analyses.[10,18,25] However, wall thickness sig-

Address correspondence to Giampaolo Martufi, Department of Civil Engineering, Schulich School of Engineering, University of Calgary, 2500 University Drive NW, Calgary, AB T2N 1N4, Canada. Electronic mail: gmartufi@ucalgary.ca

nificantly affect stress prediction and may provide a better correlation between biomechanical based indices and clinical outcomes.[36,40] ILT is present in nearly all AAA formations of clinically relevant size.[16] The presence of ILT affects aortic wall degeneration as well as wall stress.[50] ILT is a source of proteolytic enzymes[12] with ILT covered wall showing more signs of degraded elastin,[20] vascular smooth muscle cells apoptosis[22] and neovascularization from hypoxia[47] than an ILT-free wall. From a biomechanical perspective, an ILT-covered wall is thinner[20] and may exhibit diminished strength.[48] With regards to wall rupture, there is no consensus on the role of the ILT; does ILT increase the risk of aneurysm rupture through increased proteolytic activity[21]? Or is the risk diminished on account of a buffer effect of the ILT against wall stress[48]? Within this work we hypothesize that local wall thickness as well as the amount of ILT coverage at each site provide insight into the degree of disorganization of fibrous proteins in the tissue and may be used as a surrogate index to classify the local mechanical properties of the wall. In order to test this hypothesis we measured ultimate strength from *ex vivo* uniaxial tensile tests of aortic samples with different wall thickness and ILT coverage and we assessed the elastic material properties of the wall by fitting the curves obtained from the tensile tests to a histo-mechanical constitutive model.[27] We obtained a classification of the local mechanical properties and of the strength of the wall based on thickness of the wall and of the adjacent ILT. Finally, we applied our constitutive model to finite element simulations of a patient-derived aneurysm model and compared the results obtained with and without variable material properties along the vascular geometry.

MATERIALS AND METHODS

Tensile Testing

Samples of AAA were obtained fresh from the operating room from patients undergoing surgical repair following an ethical protocol approved by the institutional review board. The specimens were cut in the circumferential orientation with respect to the intact aorta from the area located across the midline on the anterior surface of the aneurysm (Fig. 1). Aneurysm diameter, age and sex as reported in the patient's clinical chart were collected for all specimens and the ILT thickness in the anterior region was measured from computer tomography-angiography (CT-A) scans when available. No bias to AAA patient selection was made with respect to age or sex. All tissue specimens were placed in saline, refrigerated at 4 °C, and tested within 48 h of procurement. The samples

width and thickness were measured for each specimen with a laser micrometer (Beta LaserMike, Inc, Dayton, Ohio) while sample length was measured with a manual caliper. For measuring the ILT thickness, a prolene stitch was placed on the AAA wall sample to mark the longitudinal level of the inferior mesenteric artery (IMA) or a known distance from the IMA, which was then used as a marker to link the location of the specimen with the corresponding longitudinal slice on CT images. ILT thickness was then measured directly on the corresponding slice of the patient's CT scan as the orthogonal distance between the lumen and the inner wall (Fig. 1). The tissue samples were cut to obtain specimens of approximately 22 mm × 4 mm and placed in the uniaxial tensile testing system.[8] After a short thermal equilibration period, each tissue sample was preconditioned, to eliminate the effect of hysteresis of the tissue during the test, by loading it to 7% strain and unloaded repeatedly for 10 cycles at a constant strain rate of 8.5%/min, while being continuously wetted with saline solution at 37 °C. Following preconditioning, tissue specimens were stretched until failure and load–displacement curves for each specimen were recorded. The first Piola–Kirchhoff stress was calculated as the recorded force normalized by the undeformed cross-sectional area, and the stretch was computed as the deformed length normalized by the original length of each specimen. The ultimate tensile strength (UTS) was taken as the peak stress obtained before specimen failure.
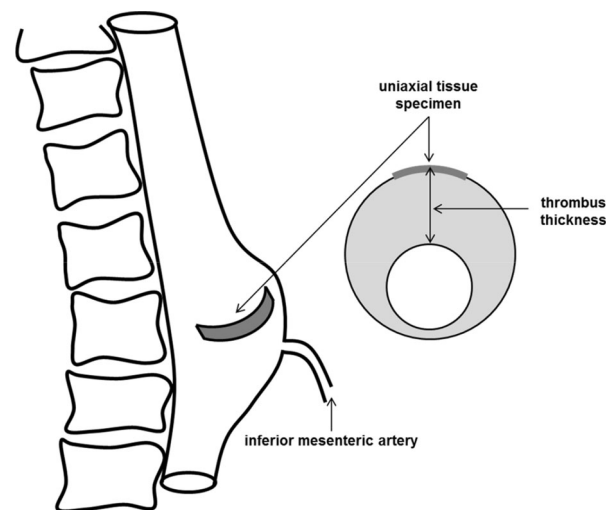

FIGURE 1. Schematic representation of the uniaxial specimen excised from the anterior region of the aneurysm. Right: cross section of the aneurysm showing the intraluminal thrombus thickness (ILT) measurement. The location of the excised specimen was localized on the computer tomography-angiography (CT-A) images using the distance between the specimen and the inferior mesenteric artery (IMA) as obtained in the operating room.

Statistical Analysis

Statistical analysis was performed with SPSS 20.0 (SPSS Inc, Chicago, Ill). Correlations between UTS and wall thickness and between ILT thickness and UTS were assessed using the Spearman's rank correlation coefficient ρ. The entire data collected were first divided over two equally sized groups based on the median of the measured wall thickness (<2.6 and >2.6 mm). Then, the subset of patients that had a CT-A scan available that allowed accurate measurement of maximum ILT thickness, were grouped based on the median of the measured maximum ILT thickness (<17 and >17 mm). The categorization yielded four subgroups: thin wall-thin ILT, thin wall-thick ILT, thick wall-thin ILT, and thick wall-thick ILT. The Mann–Whitney U test was used to compare differences in UTS between the different subgroups. For the null hypothesis test a two-sided p value lower than 0.05 was set to determine statistical significance.

Histo-Mechanical Constitutive Model of AAA Wall

The AAA wall was regarded as a fibrous collagenous tissue, where collagen fibers reinforce an isotropic matrix (composed mainly by elastin). At low strains collagen fibers are mechanically inactive and the non-collagenous material determines the vascular wall's properties. The matrix material was described by the isotropic Neo-Hookean strain energy function $\psi_{\mathrm{NH}} = \mu/2(I_1 - 3)$, where $\mu > 0$ quantified the matrix shear modulus and described the elastin-driven low stress response of the tissue, and I_1 denoted a strain invariant.[34] Each collagen fiber was assembled from bundles of collagen fibrils with different undulations mutually cross-linked by proteoglycans (CFPG-complex). The constitution of the CFPG-complex was defined by a virtually linear stress–strain response and a triangular probability density function (PDF) that defines the relative amount of engaged collagen fibrils when exposing the collagen fiber to a stretch λ.[27] Consequently, the limits of the triangular PDF $\lambda_{\min}$ and $\lambda_{\max}$ characterize the degrees of waviness of the collagen fibrils and the transition between low and high stress response. Elastin is reduced and fragmented in AAA tissue[20,38]; therefore its recoil effect decreases. This justified the setting of $\lambda_{\min} = 1$, such that $\lambda_{\max}$ entirely characterizes the undulation of collagen fibrils. Considering an incompressible collagen fiber, these assumptions yield analytical expression for the collagen fiber's Cauchy stress[27]:

$$\sigma(\lambda) = \begin{cases} 0, & 0 < \lambda \leq 1 \\ \frac{2k}{3(\lambda_{\max}-1)^2}\lambda(\lambda-1)^3, & 1 < \lambda \leq (\lambda_{\max}+1)/2 \\ k\lambda\left[\lambda - \frac{2(\lambda-\lambda_{\max})^3}{3(\lambda_{\max}-1)^2} - \frac{\lambda_{\max}+1}{2}\right], & (\lambda_{\max}+1)/2 < \lambda \leq \lambda_{\max} \\ k\lambda\left(\lambda - \frac{\lambda_{\max}+1}{2}\right), & \lambda_{\max} < \lambda < \infty \end{cases}$$

(1)

with k denoting the stiffness of the CFPG-complex and characterizing the collagen-driven response at high strain. Following the micro-fiber concept[24] the macroscopic Cauchy stress was defined by a superposition of individual collagen fiber contributions.[27] The above-outlined constitutive model was implemented in the finite element software FEAP (vs. 8.2, University of California at Berkeley, CA, USA) at the integration points of elements using a Q1P0 mixed FE formulation.[27] Details regarding the model and its numerical implementation are reported in Martufi and Gasser, 2011.[27]

Model Parameter Estimations

A single cubic tissue element was used to estimate the model material parameters μ, k and the structural parameter $\lambda_{\max}$ of the constitutive model from the results derived from the uniaxial tensile test. A constant collagen fiber density $\rho_0 = 1.35/4\pi\,sr^{-1}$ was prescribed with the same density in all directions. The clear physical meaning of the model parameters introduced allowed their straightforward identification by manual adjustments.[27]

Patient-Specific Case Study

Aneurysm Reconstruction

The geometry for a patient-specific AAA, obtained following informed consent according to institutional ethical guidelines, was reconstructed from CT-A data between the renal arteries and 1.5 cm distal to the iliac bifurcation (A4research, VASCOPS GmbH).

Wall Thickness and ILT Thickness Estimation

A suite of routines (MatLab, The MathWorks) was used to segment the lumen, the outer and inner wall of the vessel.[26,41] AAA wall thickness was estimated as minimum distance between the inner and outer wall, while ILT thickness was estimated as minimum distance between inner wall and lumen. A set of 72 equally-spaced thickness values for each CT-A image was extracted, resulting in a node-based wall thickness and ILT thickness distribution illustrated in Fig. 7. Details regarding the image segmentation process and the accuracy of the wall thickness measurement are given elsewhere.[26,41]

Finite Element Discretization

For the wall, a finite element discretization was created with a constant thickness of 2 mm (5111 Q1P0 hexahedral elements). A single element across the thickness was used; hence, the bending effects from inhomogeneous stress across the wall were neglected.

TABLE 1. Summary of patient data and mean population constitutive model parameters for abdominal aortic aneurysm (AAA) tissue samples grouped for wall and intraluminal thrombus thickness (ILT).

Patients data						Mechanical parameters			Structural parameter
Age (years)	Diameter (mm)	Wall thickness (mm)	ILT thickness (mm)	Specimens	Patients	UTS (kPa)	μ (kPa)	k (kPa)	λ_{max}
AAA tissue w/thin wall									
76 ± 10	71 ± 21	2.1 ± 0.37	–	17	14	545 ± 280	50 ± 17.8	6700 ± 4039.1	1.10 ± 0.06
AAA tissue w/thick wall									
72 ± 10	70 ± 21	3.31 ± 0.70	–	17	13	422 ± 237	10 ± 4.3	5800 ± 3699.9	1.12 ± 0.05
AAA tissue w/thin ILT									
70 ± 12	62 ± 10	2.62 ± 0.83	19 ± 4	7	5	658 ± 325	50 ± 20.3	7500 ± 4405.7	1.07 ± 0.07
AAA tissue w/thick ILT									
73 ± 7	63 ± 14	2.79 ± 1.00	32 ± 4	8	7	320 ± 141	5 ± 3.5	3500 ± 2477.9	1.07 ± 0.04

No difference ($p > 0.05$) in age or diameter was noted between the abdominal aortic aneurysm (AAA) tissue with thin and thick wall and between the AAA tissue with thin and thick intraluminal thrombus (ILT). No difference ($p > 0.05$) in wall thickness was measured between AAA tissue with thin and thick ILT. Mean values with standard deviation are presented.

TABLE 2. Summary of patient data and mean population constitutive model parameters for the abdominal aortic aneurysm (AAA) wall obtained considering the combined effect of wall and intraluminal thrombus (ILT) thickness.

Patients data						Mechanical parameters			Structural parameter
Age (years)	Diameter (mm)	Wall thickness (mm)	ILT thickness (mm)	Specimens	Patients	UTS (kPa)	μ (kPa)	k (kPa)	λ_{max}
AAA tissue w/thin wall and thin ILT									
71 ± 15	68 ± 13	1.83 ± 0.38	17 ± 0.5	3	2	772 ± 295	50 ± 24.6	7800 ± 5745.4	1.04 ± 0.10
AAA tissue w/thin wall and thick ILT									
73 ± 6	59 ± 11	2 ± 0.24	32 ± 5.0	4	3	388 ± 134	5 ± 10.0	3600 ± 1637.1	1.04 ± 0.03
AAA tissue w/thick wall and thin ILT									
69 ± 11	58 ± 4	3.2 ± 0.45	21 ± 5.0	4	3	573 ± 361	40 ± 6.4	7400 ± 3890.7	1.12 ± 0.03
AAA tissue w/thick wall and thick ILT									
74 ± 9	68 ± 18	3.6 ± 1.10	32 ± 4.0	4	4	334 ± 254	5 ± 2.0	3900 ± 3349.6	1.12 ± 0.04

Mean values with standard deviation are presented.

For the ILT, a solid mesh with a total of 9167 Q1P0 hexahedral elements was used.

Wall Mesh Modification

The hexahedral elements obtained through segmentation in VASCOPS were redefined to account for the location-based wall thickness. To do so, the normal to each surface defined by the outer face of the hexahedral wall elements was computed.[2] For every node, a new normal was then estimated by multiplying the normal unit vector by the corresponding element's thickness value, where a weight inverse to the distance between the node and the center of the element was used to obtain one representative thickness for each node. Finally the new hexahedral elements with local varying thickness were created based on the computed local nodal wall thickness.

Wall Material Properties Assignment

A discrete categorization for material properties was used where each element was considered as belonging to one of the four categories detailed in Table 2. The median of the wall thickness (1.35 mm) and ILT thickness (6.17 mm) computed on the patient specific model were used to identify the four categories.

Wall Strength Assignment

The same procedure as for the material properties assignment was followed to assign local wall strength using the mean values of the experimentally measured UTS corresponding to four categories.

Finite Element Analysis

Five simulations were performed on the same geometry considering: (a) the standard constant wall thickness of 2 mm with homogeneous material properties (average material properties were used as obtained from our experiments: $\mu = 40$ kPa, $k = 6800$ kPa, $\lambda_{max} = 1.12$) with and without ILT; (b) the variable wall thickness distribution as obtained from CT-A with homogeneous material properties, with and without ILT; and (c) the variable wall thickness distribution with
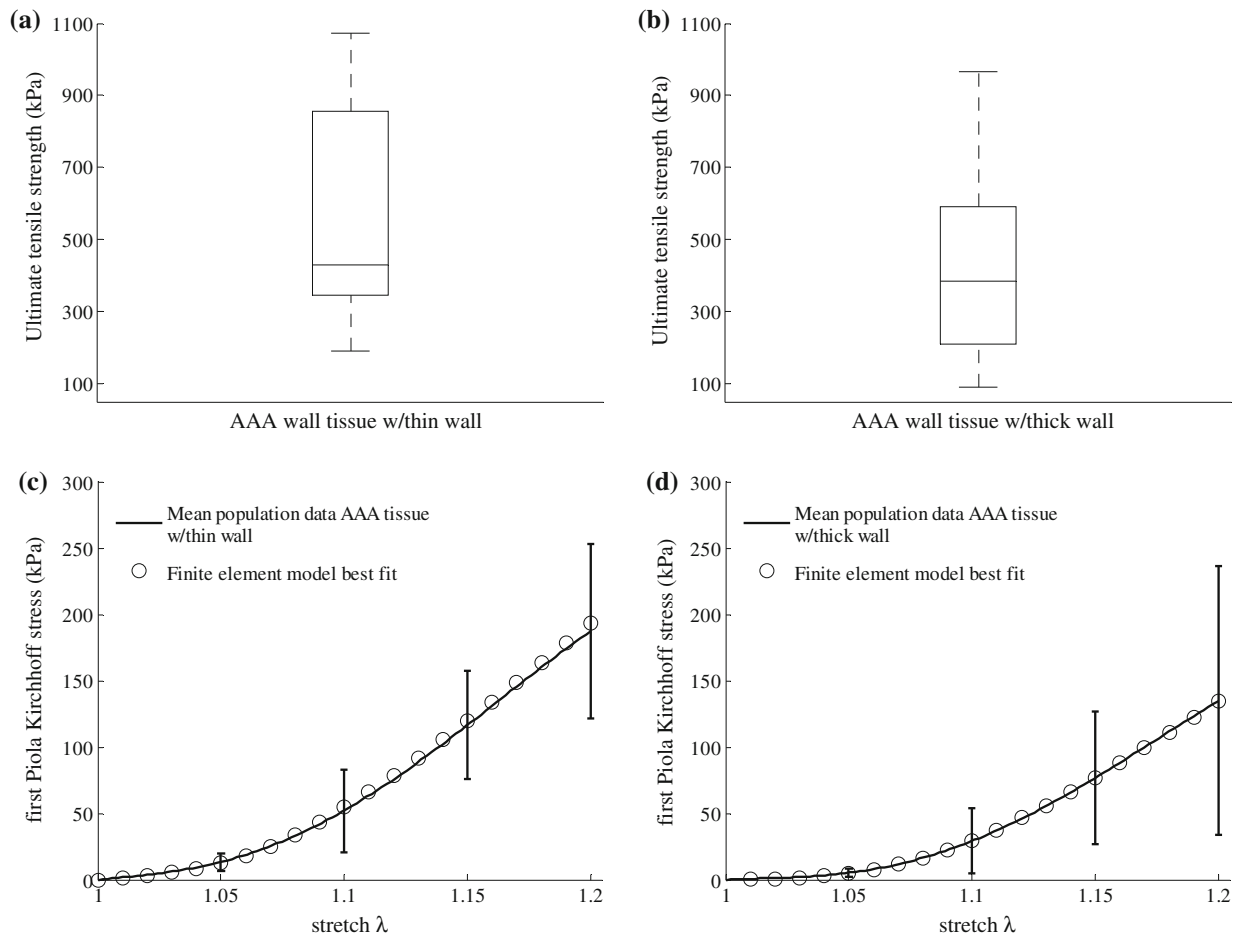
FIGURE 2. Differences in mechanical properties between Abdominal Aortic Aneurysm (AAA) samples with thin and thick wall. (a) and (b) Ultimate tensile strength (UTS); (c) and (d) Macroscopic constitutive response of the AAA wall under simple tension. Best fit finite element results (open circles) according to the multi-scale constitutive model are shown for each of the mean-population data (lines) derived from the sample cohort. Error bars represent standard deviation at the stretch values of 1.05, 1.10, 1.15, and 1.20.

non-homogeneous material properties with ILT. A mean arterial blood pressure of 100 mmHg (13.33 kPa) was applied to the luminal surface and the finite element models were fixed at the bottom and top surfaces. No contact with the surrounding organs was considered. The arterial wall was modeled as described above and the ILT tissue was modeled using one parameter Ogden-like strain energy function with the constitutive parameter set to 2.11 kPa.[15]

Rupture Potential Index Calculation

The local RPI was evaluated as the ratio between the local wall stress and the estimated local tissue strength.[14,45]

Stress Predictions Comparison

A comparison of stress predictions using finite element models with different complexities was made. In details, the Wilcoxon signed rank test was used to compare stress distributions computed with and without considering ILT. The Friedman's test was used to compare stress distributions predicted using homogenous material properties with constant and patient-specific wall thickness, and by using non-homogenous material properties with patient-specific wall thickness. For the null hypothesis test a two-sided p value lower than 0.05 was set to determine statistical significance.

RESULTS

A total of thirty-four AAA specimens were obtained from twenty-seven patients (aged 74 ± 10 years; AAA diameter, 62 ± 21 mm). Fifteen AAA specimens were harvested from twelve patients (aged 70 ± 12 years; AAA diameter, 70 ± 12 mm), which had a CT-A scan available that allowed measurement of maximum ILT thickness. Patient's data, mean population mechanical and structural parameters are summarized in Tables 1 and 2.
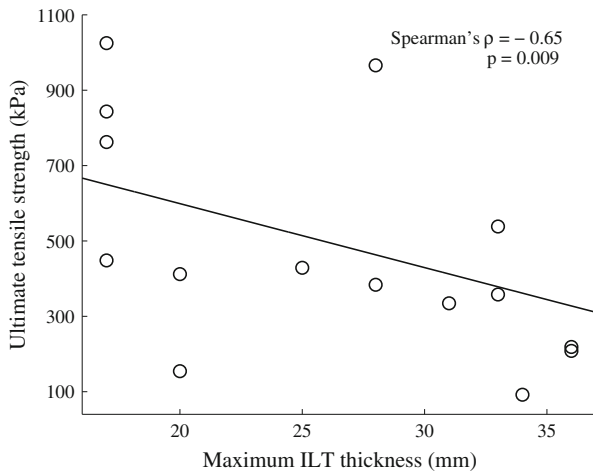
FIGURE 3. Correlation between maximum intraluminal thrombus (ILT) thickness and ultimate tensile strength (UTS). The regression line is shown for all data in the plot.

Effect of Wall Thickness on AAA Wall Tissue

There was a significant negative correlation between UTS and wall thickness (Spearman's $\rho = -0.41$, $p = 0.016$). The AAA tissue with thin wall (AAA$_{tW}$) exhibited higher values of UTS when compared to AAA tissue with thick wall (AAA$_{TW}$), i.e., 545 ± 280 vs. 422 ± 237 kPa, respectively (Figs. 2a and 2b), although the difference was not statistically significant ($p = 0.44$). Figures 2c and 2d show the mean population data for AAA$_{tW}$ and AAA$_{TW}$ groups with the finite element model best fit. The fitted values for the matrix shear modulus μ dramatically decrease from 50 to 10 kPa for the thin and thick wall respectively, while the CFPG-complex stiffness for the AAA$_{TW}$ group was just slightly lower than the one for AAA$_{tW}$ specimens (5800 vs. 6700 kPa). See Table 1 for the complete data.
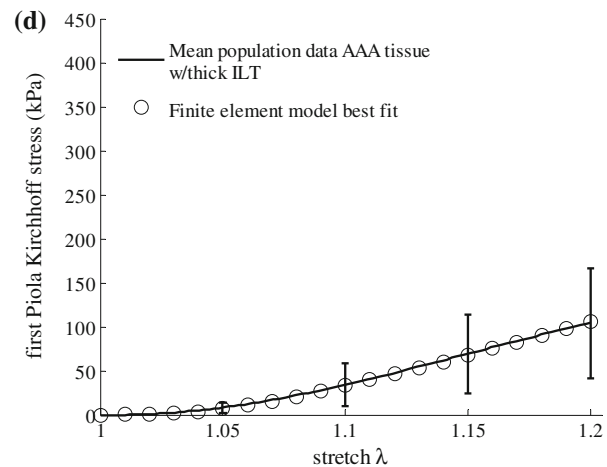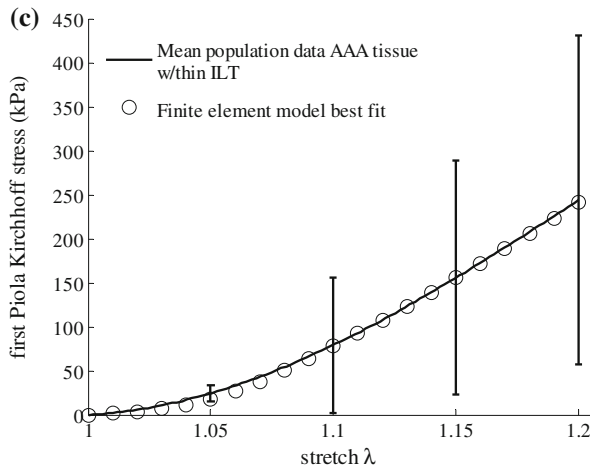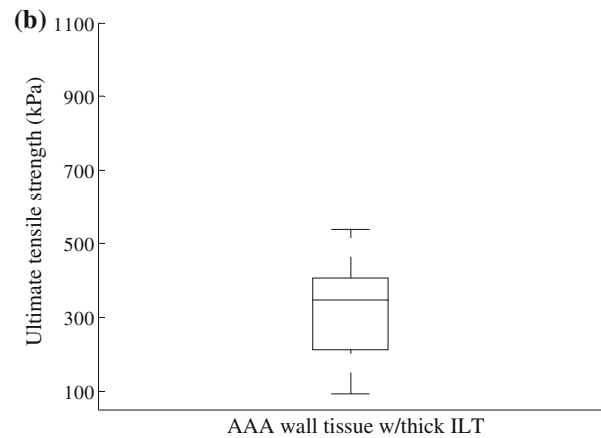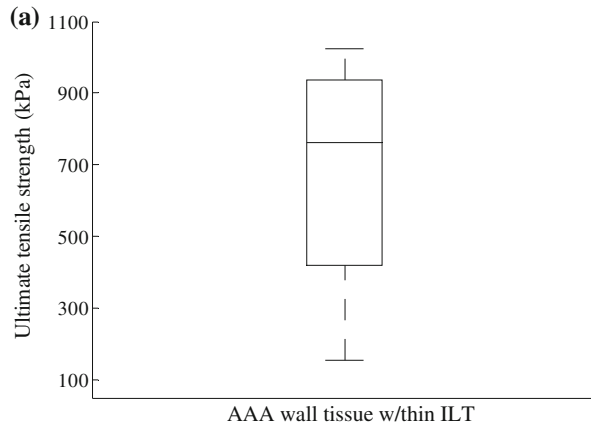

FIGURE 4. Differences in mechanical properties between wall samples adjacent to thin or thick Intraluminal thrombus (ILT). (a) and (b) Ultimate tensile strength (UTS); (b) and (c) Macroscopic constitutive response of the abdominal aortic aneurysm (AAA) wall under simple tension. Best fit finite element results (open circles) according to the multi-scale constitutive model are shown for each of the mean-population data (lines) derived from the sample cohort. Error bars represent standard deviation at the stretch values of 1.05, 1.10, 1.15, and 1.20.
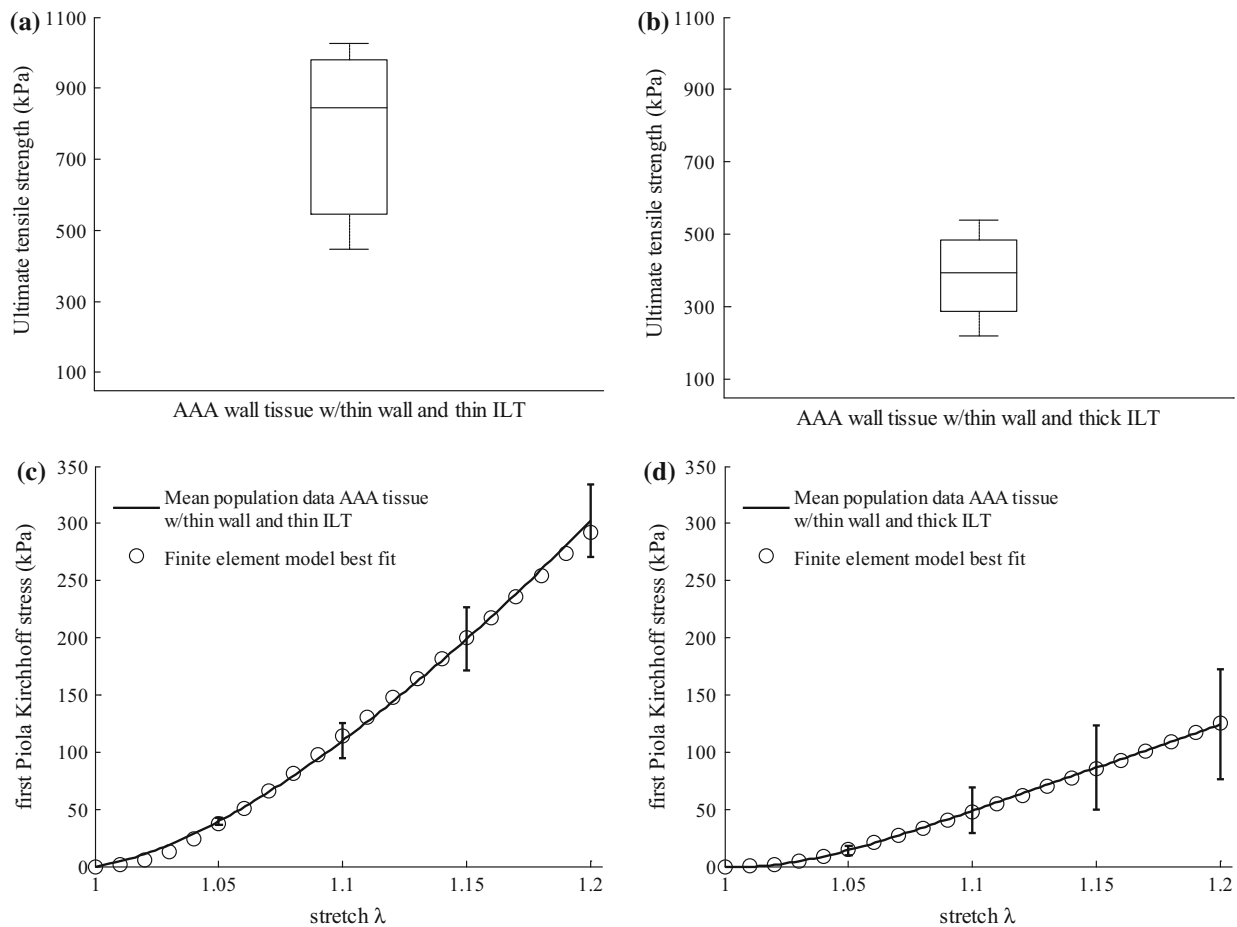
FIGURE 5. Combined effect of wall thickness and intraluminal thrombus (ILT) thickness on the mechanical properties of abdominal aortic aneurysm (AAA) wall. (a) and (b) Ultimate tensile strength for AAA thin wall with thin (a) and thick (b) ILT. Macroscopic constitutive response of the AAA thin wall with thin (c) and thick (d) ILT under simple tension. Best fit finite element results (open circles) according to the multi-scale constitutive model are shown for each of the mean-population data (lines) derived from the sample cohort. Error bars represent standard deviation at the stretch values of 1.05, 1.10, 1.15, and 1.20.

Effect of ILT Thickness on AAA Wall Tissue

UTS had a strong negative correlation with the maximum ILT thickness (Spearman's $\rho = -0.65$, $p = 0.009$, Fig. 3). The tensile strength of the AAA tissue covered with thick ILT (AAA_{TI}) was found to be significantly lower than that covered with thin ILT (AAA_{tI}), i.e., 320 ± 141 vs. 658 ± 325 kPa, respectively ($p = 0.037$; Figs. 4a and 4b). The mean population data for the AAA_{tI} and AAA_{TI} groups with the FE model best fit are shown in Figs. 4c and 4d. The matrix shear modulus μ was ten times lower for AAA_{TI} samples as compared with the AAA_{tI} group (5 vs. 50 kPa). A decrease of more than 50% in CFPG-complex stiffness was recorded in the mean population data (3500 vs. 7500 kPa for AAA_{TI} and AAA_{tI} respectively).

Combined Effect of Wall Thickness and ILT on AAA Wall Tissue

The group with thin wall and thin ILT (AAA_{tWtI}) exhibited the highest UTS (772 ± 295 kPa). For AAA tissues with thin wall, an increase in maximum ILT thickness from 17 to 32 mm caused a 54% decrease in tissue strength, with a measured UTS of 388 ± 134 kPa in the group with thin wall and thick ILT (AAA_{tWTI}). The μ and k parameters of the constitutive model were reduced from 50 to 5 kPa and from 7800 to 3600 kPa, for the AAA_{tWtI} and AAA_{tWTI} groups, respectively. The UTS of thick AAA wall sample with thin ILT (AAA_{TWtI}) was found to be lower than the one for the AAA_{tWtI} group (573 ± 361 kPa vs. 772 ± 295 kPa). The UTS reached its minimum (334 ± 254 kPa) in tissue samples where a thick ILT was deposited on a thick wall (AAA_{TWTI} group). The fitted values for the μ parameter were 40 and 5 kPa for the AAA_{TWtI} and AAA_{TWTI}, respectively, with a decrease in CFPG-complex stiffness close to 50% (7400 kPa for AAA_{TWtI} vs. 3900 for AAA_{TWTI}). None of the differences in UTS reported for the subgroups analysis of the combined effect reached statistical significance, possibly due to the
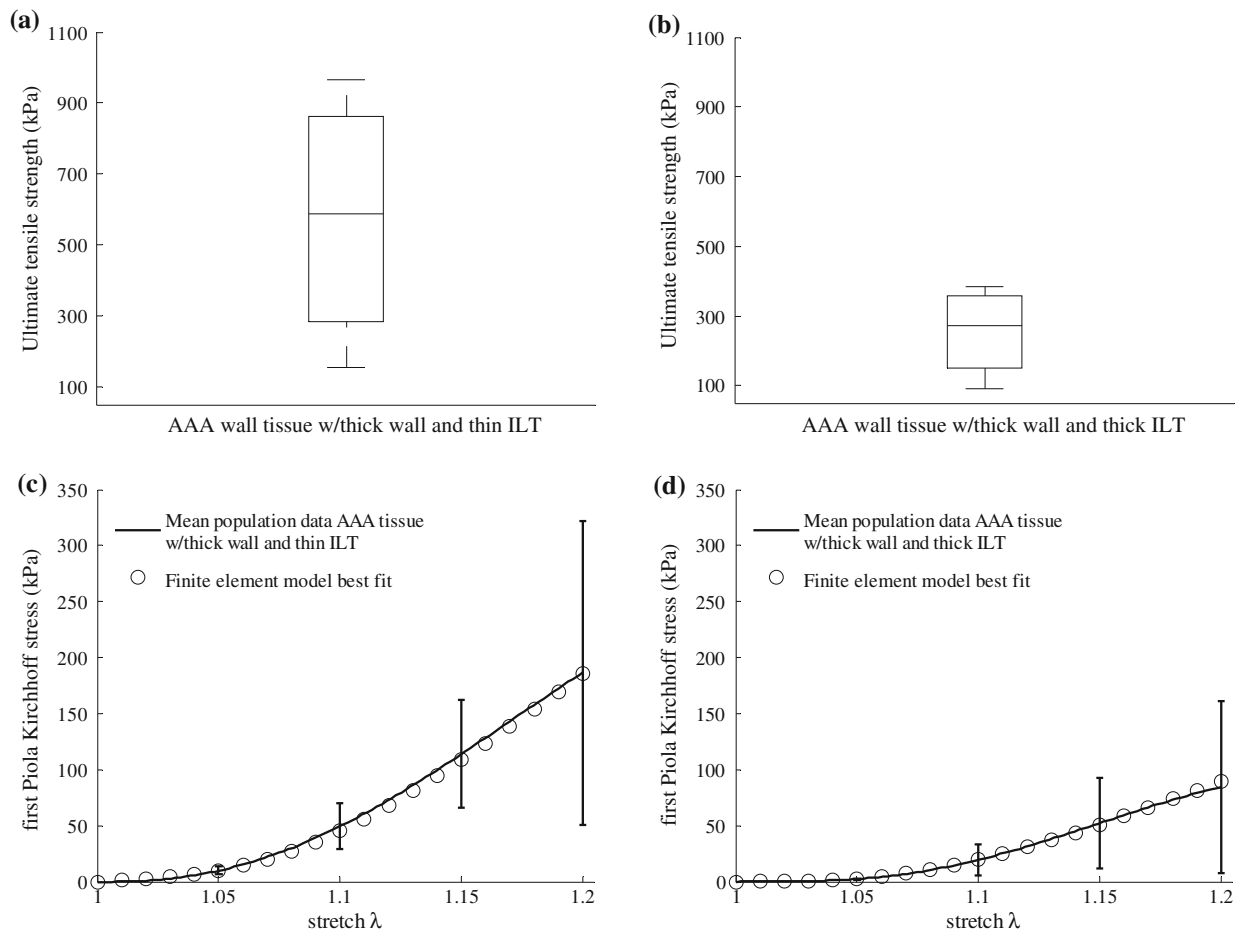
FIGURE 6. Combined effect of wall thickness and intraluminal thrombus (ILT) thickness on the mechanical properties of abdominal aortic aneurysm (AAA) wall. Ultimate tensile strength (UTS) for AAA thick wall with thin (a) and thick (b) ILT. Macroscopic constitutive response of the AAA thick wall with thin (c) and thick (d) ILT under simple tension. Best fit finite element results (open circles) according to the multi-scale constitutive model are shown for each of the mean-population data (lines) derived from the sample cohort. Error bars represent standard deviation at the stretch values of 1.05, 1.10, 1.15, and 1.20.

small sample size. See Figs. 5 and 6 and Table 2 for the complete data.

Patient-Specific Case Study

The maximum principal Cauchy stress distribution obtained using locally varying wall thickness and non-homogenous material properties as given in Table 2, is plotted in Fig. 7. Areas with high stresses were located at ILT-free regions corresponding with thin AAA wall and at areas with thick wall covered with thin ILT (Fig. 7). The measured PWS was of 311 kPa and was located in the anterior part of AAA slightly above the location of the maximum diameter, where a wall thickness of 1.34 mm covered with a 4 mm ILT was recorded. Concentrated spots of low ultimate strength were localized in the anterior part of the AAA sac, where both thin and thick wall were measured and a medium-sized ILT was deposited (Fig. 7). A large area

of low UTS interested the posterior part of the AAA, where most of the ILT was deposited (Fig. 7). The risk of rupture was distributed in a complex manner with large local variability. Multiple regions of high rupture potential could be identified. The estimated maximum RPI was 0.57 and was localized in correspondence with the highest wall stress and low wall strength.

Effect of Modeling Assumptions on the Stress Prediction

The stress distribution computed using homogenous material properties and a constant wall thickness of 2 mm (median 81.5 kPa, interquartile range (IQR), from 50.9 to 116.8 kPa) as well as that obtained with variable wall thickness (median 71.2 kPa, IQR, from 41.9 to 113.5 kPa) were found to be significantly different (Friedman test $p < 0.001$, Fig. 8) than that computed using non-homogenous material properties and variable wall thickness (median 68.5 kPa, IQR,
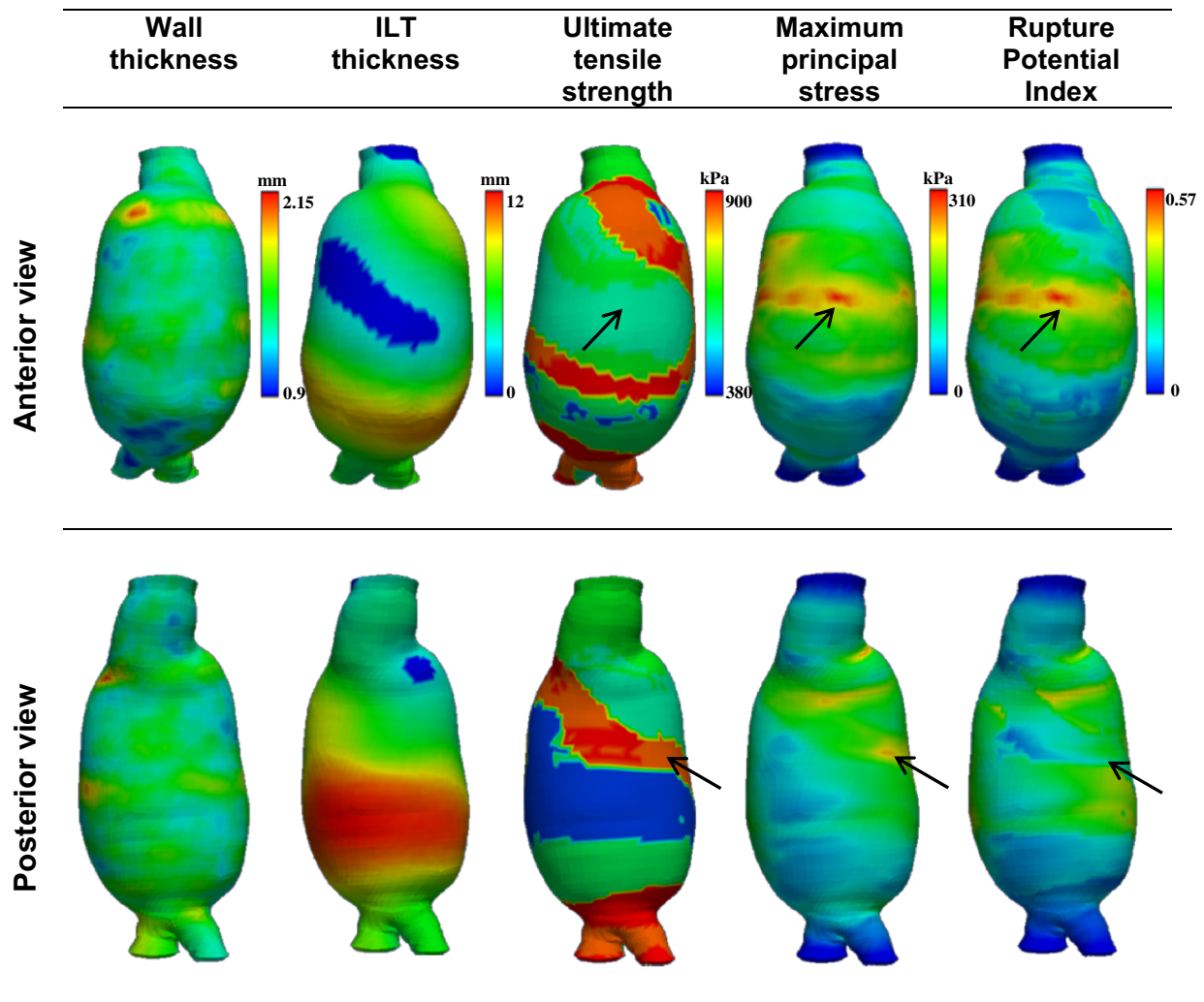
FIGURE 7. Contour plots of wall and intraluminal thrombus (ILT) thickness obtained from computer tomography-angiography (CT-A), ultimate tensile strength (UTS) computed using the categorization reported in Table 2, maximum principal Cauchy stress obtained from finite element predictions using the variable material properties given in Table 2 and rupture potential index (RPI) computed at each of the mesh nodes as the ratio between stress and strength. Top: anterior view. Bottom: posterior view. The arrows in the anterior view point to a location where low tissue strength co-localizes with high mechanical stress giving rise to a high risk of rupture (high RPI value). The arrows in the posterior view point to a location where high mechanical stress co-localizes with high tissue strength resulting in a lower risk of rupture (low RPI value).

from 40.1 to 111.3 kPa). Additionally, modeling regionally varying wall thickness but assuming homogenous material properties throughout reduced the magnitude and changed the location of the PWS. In details, the PWS predicted by using homogenous material properties and variable wall thickness was 280 kPa and was located in the anterior-lateral part of AAA, where an ILT-free wall of 1.35 mm was measured. An ulterior decrease in PWS to the value of 260 kPa was recorded when the assumptions of constant wall thickness and homogenous material properties were made (Fig. 8). Not including ILT in the biomechanical model significantly increased (Wilcoxon signed rank test $p < 0.001$) the median stress from 81.5 to 162.9 kPa (IQR, from 106.9 to 208.9 kPa) when

using constant wall thickness with homogenous material properties (Fig. 8). Using patient-specific wall thickness distribution with homogenous material properties without including ILT in the biomechanical model resulted in a stress increase (Wilcoxon signed rank test $p < 0.001$) from 71.2 to 255.3 kPa (IQR, from 154.2 to 329.4 kPa) with a PWS of 460 kPa located in the posterior-lateral side of the AAA sac where a thin wall of 1.24 mm was measured (Fig. 8).

DISCUSSION

Abdominal aortic aneurysms are traditionally considered to result from irreversible pathological remod-
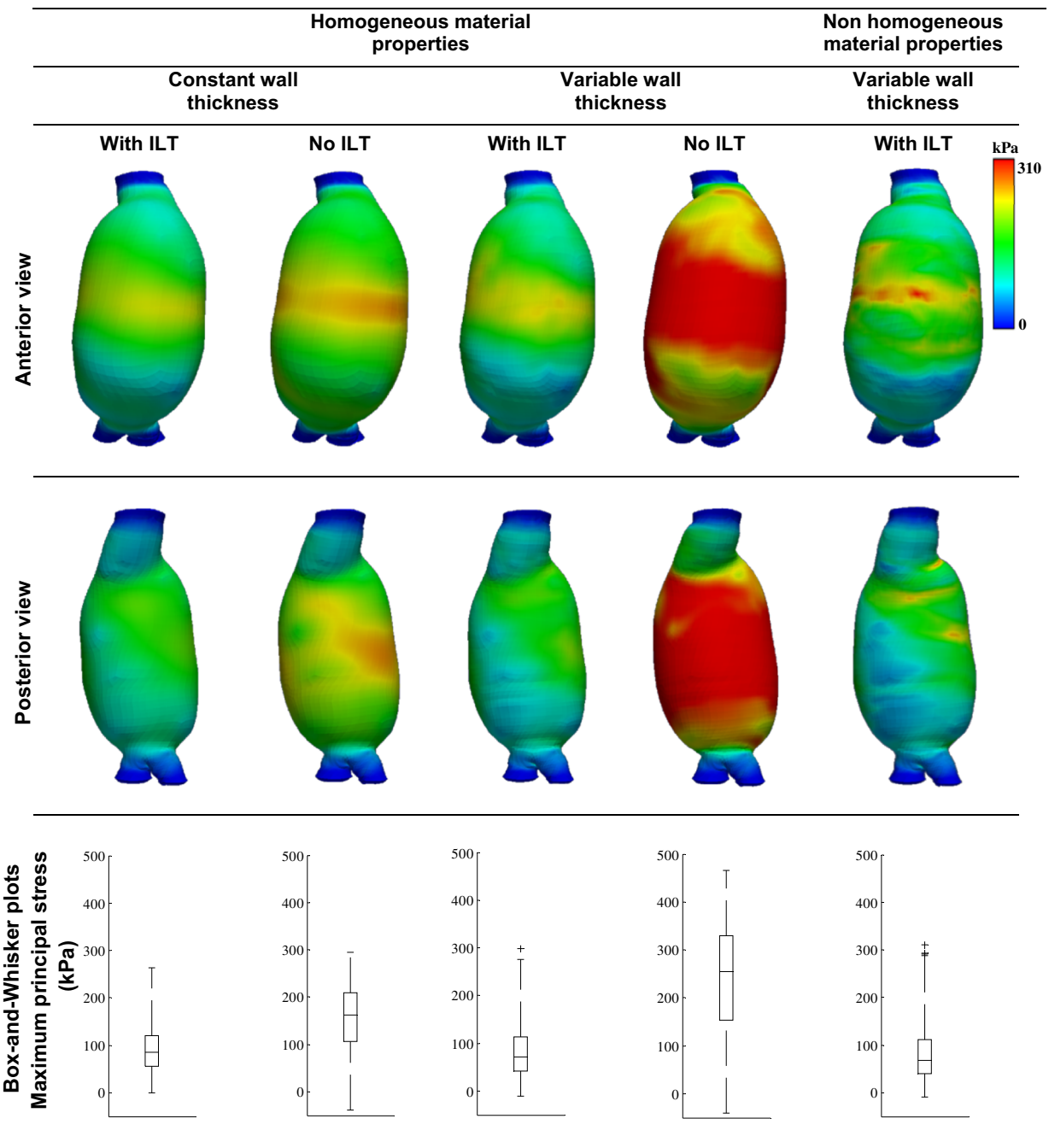
FIGURE 8. Comparison of stress prediction obtained using homogenous material properties with constant and variable wall thickness, with and without intraluminal thrombus (ILT), and using non-homogenous material properties with variable wall thickness and ILT. Top: anterior view. Center: posterior view. Bottom: box-and-whisker plot of the maximum principal Cauchy stress.

eling of the extracellular matrix and structural degradation of the aortic wall. It is widely accepted that loss of elastin triggers initial dilatation, while collagen turnover promotes enlargement. If left untreated, AAAs may progress toward further enlargement and will eventually rupture. Although it is unknown whether structural and fluid-mechanical stresses directly influence biological

activity, a potential link between high wall stress and accelerated metabolism in aortic aneurysm wall has been shown.[31] With increasing wall stress, more damage may occur in the AAA wall, leading to disorganization of fibrous proteins and strength reduction (weakening). The presence of areas with high stress co-localized with low tissues strength (see Fig. 7) recorded within this

work leads further credibility to the hypothesis of a stress mediated wall weakening process. This study confirmed the reported decrease in tissue strength (weakening) with increasing wall thickness[8] and suggested that AAA tissues with different wall thickness may exhibit differences in their mechanical behavior. The observed decrease of collagen stiffness with increasing wall thickness supports the hypothesis of wall thickening being mediated by accumulation of non load-bearing components rather than by production of load-bearing collagenous fibers.[37] The increased number of inflammatory cells and macrophage infiltration, characteristic of thick wall regions,[11,23] suggests the existence of high proteolytic activity that leads to thicker walls being weaker.[30,32] Conversely, thin wall adjacent to thick ILT suggest an imbalance in the production-degradation of tissue constituents, with more matrix being degraded than new formed. Consequently, the thickness of the aorta may be regarded as a surrogate index of structural degeneration, with both thin aortas corresponding to thick ILT and thick walls exhibiting reduced strength. An ILT is found in nearly 75% of all AAAs.[16] ILT is an active and complex biological entity,[1] which creates a hypoxic environment[47,49] and may lead to a compensatory inflammatory response that increases the proteolytic activity in the wall[30,32] with subsequent local wall weakening. Within our study an increase in ILT deposition from 19 to 32 mm resulted in an AAA wall 50% weaker and in a reduction of elastin content and collagen stiffness. Early studies have shown that macrophages exposed to hypoxia exhibit enhanced bioreactivity,[5] with subsequent increase in elastase production[3] consistent with our observed 90% decrease in elastin content from walls covered by thin ILT and the ones covered by thick ILT. Moreover, the availability of oxygen affects both the quantity and quality of extra-cellular matrix synthesis.[19,42] In other words, collagen synthetized by fibroblasts exposed to hypoxic conditions may be reduced[19,42] or abnormal[42] leading to a reduction of collagen "stiffness" which is consistent with our findings, i.e., 7500 kPa for thin ILT and 3500 kPa for thick ILT.

The greatest limitation of this study is the limited number of specimens available for the different categories; the ongoing shift from open surgical to minimally invasive aneurysm repair limits this tissue source. The limited sample number may also be the reason why we found a significant linear inverse correlation between wall thickness and UTS, while at the same time our two groups (thick and thin) failed to reach statistical difference. This occurrence underlies the importance of looking at other factors that influence wall properties (such as ILT thickness and biologically mediated weakening). Second, the finite element simulations did not account for anisotropy of the aortic wall tissue and considered only the passive response of vascular tissue, i.e., any tissue remodeling has been suppressed.[28] Third, the assignment of material properties could be improved considering a continuous distribution of material properties instead of a discrete categorization. Fourth, the impact of modeling variable wall thickness and ILT was assessed only with regards to its effects on the stress and RPI predictions, and not to its relationship with the clinical outcome. A prospective clinical study would be required to evaluate if the inclusion of locally variable wall thickness and ILT into models of AAAs will improve their ability to predict clinical outcomes. Finally, histological and histochemical analysis should be performed on the collected tissue samples and a correlation between the mechanical environment, geometrical measures and the underlying histological structure should be made.

CONCLUSIONS

Quantifying the regional variations of wall thickness as a simple geometric feature of the vessel[36,40] may be a confounding factor when the objective is the assessment of the AAA rupture risk. This study clearly showed that wall thickness plays a dual role in the evaluation of aneurysm wall stresses and rupture risk. On the one hand, a thicker AAA wall may suggest severe inflammation and accumulation of non load-bearing tissue components that locally reduce the wall strength predisposing the wall to high risk of rupture. On the other hand, localized thin-walled regions are expected to exhibit high stress concentration and therefore represent areas at high risk of rupture. Additionally as ILT deposits, the stress-shielding effect of the thrombus may be overcome by the inflammatory process with the ultimate result of a locally weak wall, prone to rupture. Local thickness of the wall and local ILT coverage may be used as surrogate measures of the local mechanical properties of the wall, and therefore, are possible candidates to improve the specificity of AAA wall stress and rupture risk evaluations.

REFERENCES

[1]Adolph, R., D. A. Vorp, D. L. Steed, M. W. Webster, M. V. Kameneva, and S. C. Watkins. Cellular content and permeability of intraluminal thrombus in abdominal aortic aneurysm. *J. Vasc. Surg.* 5:916–926, 1997.

[2]Belytschko, T., I. L. Jerry, and C. S. Tsay. Explicit algorithms for the nonlinear dynamics of shells. *Comput. Methods Appl. Mech.* 42:225–251, 1984.

[3]Campbell, E. J., and M. S. Wald. Hypoxic injury to human alveolar macrophages accelerates release of previously bound neutro-phil elastase: implications for lung connective tissue injury including pulmonary emphysema. *Am. Rev. Respir. Dis.* 127:631–635, 1983.

[4]Choksy, S. A., A. B. Wilmink, and C. R. Quick. Ruptured abdominal aortic aneurysm in the Huntingdon district: a 10-year experience. *Ann. R. Coll. Surg Engl.* 81:27–31, 1999.

[5]Compeau, C. G., J. Ma, K. N. DeCampos, T. K. Waddell, G. F. Brisseau, A. S. Slutsky, and O. D. Rotstein. In situ ischemia and hypoxia enhance alveolar macrophage tissue factor expression. *Am. J. Respir. Cell Mol. Biol.* 11:446–455, 1994.

[6]Darling, R. C., C. R. Messina, D. C. Brewster, and L. W. Ottinger. Autopsy study of unoperated abdominal aortic aneurysms. *Circulation* 56(2):161–164, 1977.

[7]Davies, M. J. Aortic aneurysm formation: lessons from human studies and experimental models. *Circulation* 98:193–195, 1998.

[8]Di Martino, E. S., A. Bohra, J. P. Vande Geest, N. Gupta, M. Makaroun, and D. A. Vorp. Biomechanical properties of ruptured versus electively repaired abdominal aortic aneurysm wall tissue. *J. Vasc. Surg.* 43:570–576, 2006.

[9]Fillinger, M. Who should we operate on and how do we decide: predicting rupture and survival in patients with aortic aneurysm. *Semin. Vasc. Surg.* 20(2):121–127, 2007.

[10]Fillinger, M. F., S. P. Marra, M. L. Raghavan, and F. E. Kennedy. Prediction of rupture risk in abdominal aortic aneurysm during observation: wall stress versus diameter. *J. Vasc. Surg.* 37:724–732, 2003.

[11]Folco, E. J., Y. Sheikine, V. Z. Rocha, T. Christen, E. Shvartz, G. K. Sukhova, M. F. Di Carli, and P. Libby. Hypoxia but not inflammation augments glucose uptake in human macrophages: implications for imaging atherosclerosis with 18fluorine-labeled 2-deoxy-d-glu-cose positron emission tomography. *J. Am. Coll. Cardiol.* 58(6):603–614, 2011.

[12]Folkesson, M., A. Silveira, P. Eriksson, and J. Swedenborg. Protease activity in the multi-layered intra-luminal thrombus of abdominal aortic aneurysms. *Atherosclerosis* 218:294–299, 2011.

[13]Galland, R. B., M. S. Whiteley, and T. R. Magee. The fate of patients undergoing surveillance of small abdominal aortic aneurysms. *Eur. J. Vasc. Endovasc.* 16:104–109, 1998.

[14]Gasser, T. C., M. Auer, F. Labruto, J. Swedenborg, and J. Roy. Biomechanical rupture risk assessment of abdominal aortic aneurysms: model complexity versus predictability of finite element simulations. *Eur. J. Vasc. Endovasc. Surg.* 40:176–185, 2010.

[15]Gasser, T. C., G. Görgülü, M. Folkesson, and J. Swedenborg. Failure properties of intra-luminal thrombus in abdominal aortic aneurysm under static and pulsating mechanical loads. *J. Vasc. Surg.* 48:179–188, 2008.

[16]Hans, S. S., O. Jareunpoon, M. Balasubramaniam, and G. B. Zelenock. Size and location of thrombus in intact and ruptured abdominal aortic aneurysms. *J. Vasc. Surg.* 41:584–588, 2005.

[17]Heikkinen, M., J.-P. Salenius, and O. Auvinen. Ruptured abdominal aortic aneurysm in a well-defined geographical area. *J. Vasc. Surg.* 36:291–296, 2002.

[18]Heng, M. S., M. J. Fagan, W. Collier, G. Desai, P. T. McCollum, and I. C. Chetter. Peak wall stress measurement in elective and acute abdominal aortic aneurysms. *J. Vasc. Surg.* 47:17–22, 2008.

[19]Herrick, S. E., G. W. Ireland, D. Simon, C. N. McCollum, and M. W. Ferguson. Venous ulcer fibroblasts compared with normal fibroblasts show differences in collagen but not fibronectin production under both normal and hypoxic conditions. *J. Invest. Dermatol.* 106:187–193, 1996.

[20]Kazi, M., J. Thyberg, P. Religa, J. Roy, P. Eriksson, U. Hedin, and J. Swedenborg. Influence of intraluminal thrombus on structural and cellular composition of abdominal aortic aneurysm wall. *J. Vasc. Surg.* 38:1283–1292, 2003.

[21]Kazi, M., C. Zhu, J. Roy, G. Paulsson-Berne, A. Hamsten, J. Swedenborg, U. Hedin, and P. Eriksson. 2005 Difference in matrix-degrading protease expression and activity between thrombus-free and thrombus-covered wall of abdominal aortic aneurysm. *Arterioscler. Thromb. Vasc. Biol.* 25:1341–1346, 2005.

[22]Koole, D., H. J. A. Zandvoort, A. Schoneveld, A. Vink, J. A. Vos, L. L. van den Hoogen, J. P. P. M. de Vries, G. Pasterkamp, F. L. Moll, and J. A. van Herwaarden. Intraluminal abdominal aortic aneurysm thrombus is associated with disruption of wall integrity. *J. Vasc. Surg.* 57(1):77–83, 2013.

[23]Kotze, C., A. Groves, L. Menezes, R. Harvey, R. Endozo, I. Kayani, P. Ell, and S. Yusuf. What is the relationship between 18F-FDG aortic aneurysm uptake on PET/CT and future growth rate? *Eur. J. Nucl. Med. Mol. Imaging* 38(8):1493–1499, 2011.

[24]Lanir, Y. Constitutive equations for fibrous connective tissues. *J. Biomech.* 16(1):1–12, 1983.

[25]Maier, A., M. W. Gee, C. Reeps, J. Pongratz, H. H. Eck-steinand, and W. A. Wall. A comparison of diameter, wall stress, and rupture potential index for abdominal aortic aneurysm rupture risk prediction. *Ann. Biomed. Eng.* 38:3124–3134, 2010.

[26]Martufi, G., E. S. Di Martino, C. H. Amon, S. C. Muluk, and E. A. Finol. Three-dimensional geometrical characterization of abdominal aortic aneurysms: image-based wall thickness distribution. *J. Biomech. Eng.* 31(6):061015, 2009.

[27]Martufi, G., and T. C. Gasser. A constitutive model for vascular tissue that integrates fibril, fiber and continuum levels with application to the isotropic and passive properties of the infrarenal aorta. *J. Biomech.* 44:2544–2550, 2011.

[28]Martufi, G., and T. C. Gasser. Turnover of fibrillar collagen in soft biological tissue with application to the expansion of abdominal aortic aneurysms. *J. R. Soc. Interface* 9(77):3366–3377, 2012.

[29]Martufi, G., and T. C. Gasser. Review: the role of biomechanical modeling in the rupture risk assessment for abdominal aortic aneurysms. *J. Biomech. Eng.* 135(2):021010, 2013.

[30]McMillan, W. D., B. K. Patterson, R. R. Keen, and W. H. Pearch. In situ localization and quantification of seventy-

two-kilodalton type IV collagenase in aneurysmal, occlusive, and normal aorta. *J. Vasc. Surg.* 22:295–305, 1995.

[31]Nchimi, A., J. P. Cheramy-Bien, T. C. Gasser, G. Namur, P. Gomez, L. Seidel, A. Albert, J. O. Defraigne, N. Labropoulos, and N. Sakalihasan. Multifactorial relationship between 18f-fluoro-deoxy glucose positron emission tomography signaling and biomechanical properties in unruptured aortic aneurysms. *Circ. Cardiovasc. Imaging.* 7(1):82–91, 2014.

[32]Newman, K. M., J. Jean-Claude, L. Hong, J. V. Scholes, Y. Ogata, H. Nagase, and M. D. Tilson. Cellular localization of matrix metalloproteinases in the abdominal aortic aneurysm wall. *J. Vasc. Surg.* 20:814–820, 1994.

[33]Nicholls, S. C., J. B. Gardner, M. H. Meissner, and K. Johansen. Rupture in small abdominal aortic aneurysms. *J. Vasc. Surg.* 28:884–888, 1998.

[34]Ogden, R. W. Non-linear elastic deformations. New York, NY: Dover, 1997.

[35]Raghavan, M. L., J. Kratzberg, E. M. CastrodeTolosa, M. M. Hanaoka, P. Walker, and E. S. daSilva. Regional distribution of wall thickness and failure properties of human abdominal aortic aneurysm. *J. Biomech.* 39:3010–3016, 2006.

[36]Raut, S. S., A. Jana, V. De Oliveira, S. C. Muluk, and E. A. Finol. The importance of patient-specific regionally varying wall thickness in abdominal aortic aneurysm biomechanics. *J. Biomech. Eng.* 135(8):081010, 2013.

[37]Reeps, C., A. Maier, J. Pelisek, F. Härtl, V. Grabher-Meier, W. A. Wall, M. Essler, H. H. Eckstein, and M. W. Gee. Measuring and modeling patient-specific distributions of material properties in abdominal aortic aneurysm wall. *Biomech. Model. Mechanobiol.* 12:717–733, 2012.

[38]Rizzo, R. J., W. J. McCarthy, S. N. Dixit, M. P. Lilly, V. P. Shively, W. R. Flinn, and J. S. T. Yao. Collagen types and matrix protein content in human abdominal aortic aneurysms. *J. Vasc. Surg.* 10(4):365–373, 1989.

[39]Rodriguez, J. F., G. Martufi, M. Doblare, and E. A. Finol. The effect of material model formulation in the stress analysis of abdominal aortic aneurysms. *Ann. Biomed. Eng.* 37(11):2218–2221, 2009.

[40]Shang, E. K., D. P. Nathan, R. M. Fairman, E. Y. Woo, G. J. Wang, R. C. Gorman, J. H. Gorman III, and B. M. Jackson. Local wall thickness in finite element models improves prediction of abdominal aortic aneurysm growth. *J. Vasc. Surg.*, 61(1):217–223, 2015.

[41]Shum, J., E. S. DiMartino, A. Goldhammer, D. Goldman, L. Acker, G. Patel, J. H. Ng, G. Martufi, and E. A. Finol. Semi-automatic vessel wall detection and quantification of wall thickness in CT images of human abdominal aortic aneurysms. *Med. Phys.* 37:638–648, 2010.

[42]Steinbrech, D. S., M. T. Longaker, B. J. Mehrara, P. B. Saadeh, G. S. Chin, R. P. Gerrets, D. C. Chau, N. M. Rowe, and G. K. Gittes. Fibroblast response to hypoxia: the relationship between angiogenesis and matrix regulation. *J. Surg. Res.* 84:127–133, 1999.

[43]The UK Small Aneurysm Trial Participants. Mortality results for randomised controlled trial of early elective surgery or ultrasonographic surveillance for small abdominal aortic aneurysms. *Lancet.* 352:1649–1655, 1998.

[44]Upchurch, Jr., G. R., and T. A. Schaub. Abdominal aortic aneurysm. *Am. Family Physician* 73:1198–1204, 2006.

[45]Vande Geest, J. P., E. S. Di Martino, A. Bohra, M. S. Makaroun, and D. A. Vorp. A biomechanics-based rupture potential index for abdominal aortic aneurysm risk assessment: demonstrative application. *Ann. N. Y. Acad. Sci.* 1085:11–21, 2006.

[46]Venkatasubramaniam, A. K., M. J. Fagan, T. Mehta, K. J. Mylankal, B. Ray, G. Kuhan, I. C. Chetter, and P. T. McCollum. A comparative study of aortic wall stress using finite element analysis for ruptured and non-ruptured abdominal aortic aneurysms. *Eur J. Vasc. Surg.* 28:168–176, 2004.

[47]Vorp, D. A., P. C. Lee, D. H. Wang, M. S. Makaroun, E. M. Nemoto, S. Ogawa, and M. W. Webster. Association of intraluminal thrombus in abdominal aortic aneurysm with local hypoxia and wall weakening. *J. Vasc. Surg.* 34:291–299, 2001.

[48]Vorp, D. A., and J. P. Vande Geest. Biomechanical determinants of abdominal aortic aneurysm rupture. *Arterioscler. Thromb. Vasc. Biol.* 25:1558–1566, 2005.

[49]Vorp, D. A., D. H. J. Wang, M. W. Webster, and W. J. Federspiel. Effect of intraluminal thrombus thickness and bulge diameter on the oxygen flow in abdominal aortic aneurysm. *J. Biomech. Eng.* 120:579–583, 1998.

[50]Wang, D., M. Makaroun, M. Webster, and D. A. Vorp. Effect of intraluminal thrombus on wall stress in patient specific models of abdominal aortic aneurysm. *J. Vasc. Surg.* 36:598–604, 2002.